a-b Plane Anisotropy of the Superconducting Gap in $Bi_2Sr_2CaCu_2O_8$: Scanning Tunneling Microscope Spectroscopy

K. Suzuki,[1] K. Ichimura,[1] K. Nomura,[1] and S. Takekawa[2]
[1]*Division of Physics, Hokkaido University, Sapporo 060-0810, Japan*
[2]*National Institute for Research in Inorganic Materials, Tsukuba, Ibaraki 305-0044, Japan*
(Received 25 January 1999)

We have carried out electron tunneling spectroscopy on $Bi_2Sr_2CaCu_2O_8$ single crystals with use of STM at 4.2 K. The tunneling differential conductance in the superconducting gap was observed with varying tunneling direction in the *a-b* plane. Tunneling spectra observed along directions intermediate between Cu-O and Cu-Cu directions are well fitted with the $d_{x^2-y^2}$ wave model, taking into account the **k** dependence of the tunneling transition probability. This result strongly indicates that the superconducting gap has the $d_{x^2-y^2}$ wave symmetry with line nodes along the Cu-Cu direction.

PACS numbers: 74.50.+r, 71.20.–b, 74.72.Hs

Since the discovery of high-T_c cuprates, many investigations have been carried out on the mechanism of its superconductivity. In high-T_c cuprates, it is known that the superconductivity is caused by carriers in Cu-O layers, where the on-site Coulomb repulsive interaction at a Cu site is very strong. Therefore, the attractive interaction between electrons mediated by phonon can hardly bring about Cooper pairs in contrast to conventional superconductors. We must investigate the mechanism which causes an attractive interaction between electrons in such a strong correlation system. The symmetry of the superconducting pair wave function is an important clue to the attractive interaction between electrons. Many kinds of experiments were carried out to investigate it, e.g., measurement of the magnetic field penetration depth [1], angle-resolved photoemission spectroscopy (ARPES) [2,3], and NMR relaxation rate measurement [4]. Many of them suggest that the superconducting gap of high-T_c cuprates has the *d*-wave symmetry. However, in the scanning tunneling microscope (STM) spectroscopy method, by which one can observe the electronic density of states directly with high resolution in energy, various results were reported [5–12], and those results have not converged yet. We reported that the superconducting gap is highly anisotropic in $Bi_2Sr_2CaCu_2O_8$ from STM spectroscopy measurements on single crystals [13]. In order to make more detailed discussion, we have observed tunneling differential conductance with varying tunneling direction in the *a-b* plane. In this article, we report the result of the tunneling spectra and discuss the symmetry of the pair wave function in the superconducting phase.

$Bi_2Sr_2CaCu_2O_8$ single crystals used in this study were grown by the floating-zone method. The superconducting transition temperature T_c was determined as $T_c = 87$ K from the midpoint of the resistive transition. The crystal orientation was determined by x-ray diffraction. In this article, we always denote the [100] and [110] directions as the Cu-O bonding and Cu-Cu directions in the Cu-O plane, respectively. It was ensured that these single crystals grow along the [110] direction. Clean lateral surfaces were prepared by cutting them with a razor blade in air. Surfaces perpendicular to the [100], [110], and $\Phi = 9°$, 19°, 27°, 35°, and 38° directions from the [100] direction in the Cu-O plane were obtained. We ensured that each cut surface is flat with an optical microscope. Furthermore, we observed a typical cut surface with a scanning electron microscope (SEM) and ensured its flatness. The sample was mounted into the STM unit cell filled with the low pressure helium gas for thermal exchange. A mechanically sharpened Pt-Ir alloy wire was used as the STM tip. The measurements were carried out in the vacuum tunneling configuration where the STM tip does not contact to the sample surface. Differential conductance curves were observed directly by the lock-in technique with a 1-kHz ac modulation of 1 mV superposed on the bias voltage.

Typical differential conductance curves observed at 4.2 K with varying tunneling direction in the *a-b* plane are shown together in Fig. 1. The initial tunneling current I_0 is reduced exponentially with increasing the distance between the tip and the sample surface. We found that the functional form of the tunneling curves did not depend on the tip distance except for the [100] direction. Each curve is normalized by dividing with I_0 for the bias voltage $V_0 = 100$ mV. These curves show the clear superconducting gap structure except for the [100] direction. The curve along the [100] direction shows a conductance peak structure near zero bias voltage, whose detailed structure depends on the tip distance [14]. The functional form of curves along directions intermediate between [100] and [110] varies systematically, depending on the tunneling direction as described below. First, we discuss these curves from the viewpoint of the anisotropic superconducting gap.

For each tunneling direction, differential conductance curves were observed at several positions, which were aligned at intervals of about 10 nm on the cut surface. On each cut surface, essentially the same curve was observed

 0031-9007/99/83(3)/616(4)$15.00

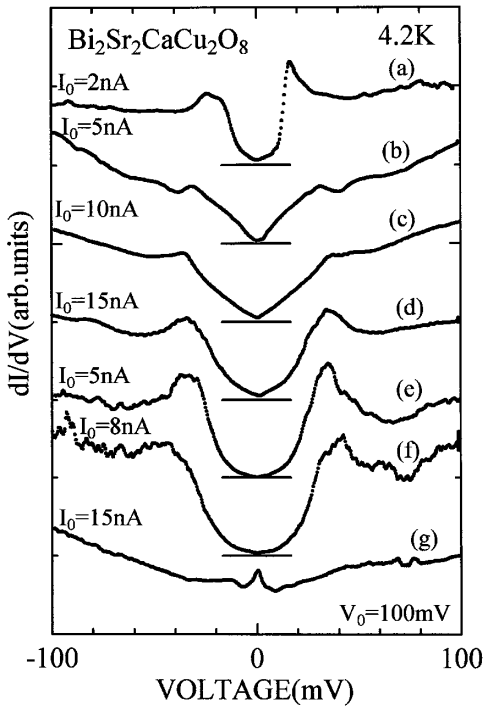

FIG. 1. Tunneling differential conductance observed at 4.2 K with varying tunneling direction in the a-b plane of $Bi_2Sr_2CaCu_2O_8$ single crystals. Curves observed along the [110] direction (a), $\Phi = 38°$ (b), 35° (c), 27° (d), 19° (e), 9° (f), and the [100] direction (g) are shown together. These curves were observed for the initial voltage $V_0 = 100$ mV. Each curve is normalized by dividing with the initial tunneling current I_0. The zero-conductance line of each curve is shifted by one division for clarity.

reproducibly irrespective of the tip position. These curves clearly show the superconducting gap structure. The gap edge is observed as an enhancement of the conductance. The conductance is reduced to almost zero near zero bias voltage. The shape of these curves is almost symmetric with respect to the Fermi level. Outside the gap edge, however, these curves do not always show the flat behavior, which is expected for the electronic density of states in the normal phase. For the curves along $\Phi = 35°$ and 38°, the conductance increases with the bias voltage and shows the so-called V-shape background as has been reported frequently [8,11]. However, we know from our experience that observed curves show the electronic density of states correctly inside the superconducting gap [13]. As shown in Fig. 1, the magnitude of the gap $\Delta_{p\text{-}p}$, where the peak-to-peak width is defined as $2\Delta_{p\text{-}p}$, increases from 31 meV to 40 meV with decreasing Φ. These values are consistent with those obtained by other groups [8–12]. The enhancement of the gap edge is reduced with increasing Φ. The functional form near zero bias voltage also varies systematically depending on the tunneling direction. For the tunneling curves along near the [100] direction like $\Phi = 9°$ and 19°, the functional form near zero bias voltage is rather flat. The curves for tunneling along near the [110] direction like $\Phi = 35°$ and 38° show the linear voltage dependence of the energy near zero bias voltage. Moreover, the curve whose functional form inside the gap edge is upwards convex is often observed along $\Phi = 35°$ or 38°. Figures 2(a) and 2(b) show curves observed at different positions, which were separated by several hundreds of micrometers on the cut surface of $\Phi = 35°$ and 19°, respectively. On each cut surface, the functional form near zero bias voltage depends on the position slightly. This is probably due to some roughness of each cut surface. The conductance curve observed most frequently for each direction is shown in Fig. 1. Accordingly, the tunneling direction dependence of the functional form described above is intrinsic. Such tunneling direction dependence of the functional form indicates that the superconducting gap is highly anisotropic in the a-b plane. This also means that we cannot neglect the dependence of the tunneling transition probability on the wave vector $\mathbf{k}$ even in STM measurement. The energy-linear dependence observed along near the [110] direction suggests that the gap has line nodes on the Fermi surface near the [110] direction. Therefore, the $d_{x^2-y^2}$-wave gap with line nodes along the [110] direction is the most suitable candidate.

We try to fit these curves to the calculated electronic density of states with the $d_{x^2-y^2}$-wave model. We examine the simplest one, in which the gap Δ depends only on the direction in $\mathbf{k}$ space, given as

$$\Delta = \Delta_0 \cos 2\theta\,, \tag{1}$$

where Δ_0 and θ are the maximum value of the superconducting gap and the angle from the maximum gap direction in $\mathbf{k}$ space, respectively. The directional dependence of the tunneling differential conductance is given as

$$\frac{dI}{dV}(V,\theta_0) \propto \int_0^{2\pi}\int_{-\infty}^{\infty} p(\theta - \theta_0) \times \mathrm{Re}\left[\frac{E - i\Gamma}{\sqrt{(E - i\Gamma)^2 - \Delta(\theta)^2}}\right] \times \left[-\frac{\partial f(E + eV)}{\partial V}\right] N(\theta)\, dE d\theta\,, \tag{2}$$

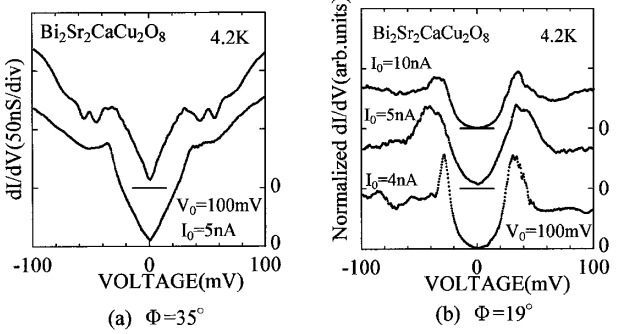

FIG. 2. Tunneling differential conductance observed at 4.2 K along $\Phi = 35°$ (a) and 19° (b). On each cut surface, curves were observed at different positions, which were separated by several hundreds of micrometers. In (b), curves are normalized at $V = 100$ mV. In each figure, the zero-conductance line of each curve is shifted by one division for clarity.

where $f(E)$ is the Fermi distribution function. We introduce the lifetime broadening parameter of the one-electron level Γ. The $\mathbf{k}$ dependence of the tunneling transition probability is taken into account by the factor $p(\theta - \theta_0)$. The parameter θ_0 is the angle of the direction perpendicular to the tunneling barrier. According to the WKB approximation [15], $p(\theta - \theta_0)$ decays exponentially as

$$p(\theta - \theta_0) = \exp[-\beta \sin^2(\theta - \theta_0)]. \quad (3)$$

The parameter β is given as

$$\beta = \sqrt{\frac{2m}{\hbar^2}} \frac{E_F}{\sqrt{U - E_F}} d, \quad (4)$$

where U and E_F are the potential height of the tunneling barrier and the Fermi energy, respectively, and d is the width of the tunneling barrier. Owing to this factor, an electron whose kinetic energy component perpendicular to the tunneling barrier is large has a large probability of tunneling. The factor $N(\theta)$ represents the anisotropy of the band dispersion and is given as

$$N(\theta) = \frac{1}{|\nabla_{\mathbf{k}} \varepsilon(\mathbf{k})|}. \quad (5)$$

According to tight-binding approximation, the dispersion relation of the two-dimensional square lattice is given as

$$\varepsilon(\mathbf{k}) - \mu_0 = -\varepsilon_0[\cos(k_x a) + \cos(k_y a)], \quad (6)$$

where μ_0, ε_0, and a are the Fermi energy in the half-filled conduction band, the bandwidth, and the lattice parameter, respectively. The direction dependence of $N(\theta)$ is sensitive to the band filling. The conduction band of $Bi_2Sr_2CaCu_2O_8$, is almost half filled with a small amount of hole doping. We assume $E_F - \mu_0 = -0.05\varepsilon_0$ for the Fermi energy E_F in the following calculation. The value of $N(\theta)$ calculated using this model has a large magnitude for the wave vector $\mathbf{k}$ around the [100] direction.

The differential conductance curves calculated for $T = 4.2$ K with this model are shown as broken curves in Fig. 3. In those fittings, we regarded θ_0, Δ_0, and Γ as fitting parameters for each direction. We fixed the parameter β as the value of 8 for all curves. The functional form near zero bias voltage of the calculated curve reproduces the flat behavior observed along near the [100] direction. The slope near zero bias voltage of the calculated curve becomes large with increasing θ_0, and the energy-linear behavior observed along near the [110] direction is reproduced. Moreover, the functional form of the curve along $\Phi = 38°$, which is upwards convex inside the gap edge, is also well reproduced. The remaining conductance near zero bias voltage is explained by the broadening parameter Γ. Small value of $\Gamma = 0.3-1.1$ meV assures the validity of the discussion about the superconducting electronic state with our tunneling curves. The variation of the enhancement of the gap edge, which is reduced with increasing Φ, is also well explained qualitatively. The gap width $\Delta_{p\text{-}p}$ in the calculated curve using the same Δ_0 becomes large with decreasing θ_0. However, the values of the measured gap $\Delta_{p\text{-}p}$ are not explained systematically with a unique value of Δ_0. This implies that the sample dependence of Δ_0 and the inhomogeneity of the sample are not negligible. The obtained values of $\Delta_0 = 30-36$ meV from the fitting are consistent with those of other tunneling experiments [8–12]. The value of $\beta = 8$, for which the transition probability decays by a factor of e^{-1} at $\theta - \theta_0 = 20°$, is relatively small. Ichimura *et al.* [16] reported the value of $\beta = 20$ from STM spectroscopy on $(BEDT\text{-}TTF)_2Cu(NCS)_2$ which is an organic superconductor with the two-dimensional electronic band. As known from Eq. (4), this difference of the value of β is probably due to the difference of the work function $U - E_F$ or the tip distance d. In Fig. 4, the fitting parameter θ_0 is plotted against Φ measured under an optical microscope. These points are almost on the straight line which intersects the origin. This means that the line node of the gap is at the [110] direction. In the above fitting, an anisotropic band dispersion is assumed. We tried the same fitting assuming an isotropic band dispersion and ensured that these curves are well explained in the same way, and the similar relation between θ_0 and Φ is obtained again. Accordingly, our conclusion of the gap anisotropy does not depend on the assumed Fermi energy. Moreover, we ensured that all the curves which are shown in Fig. 2 are also explained by the $d_{x^2-y^2}$-wave gap in the same way. As a result, the

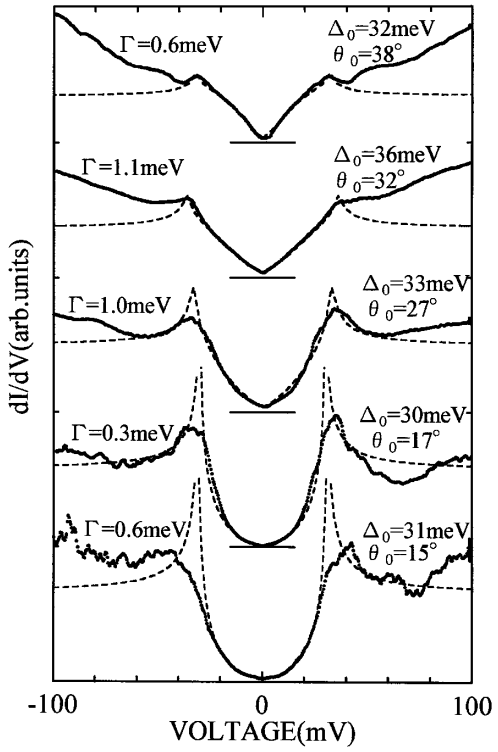

FIG. 3. The fitting of tunneling differential conductance observed along the intermediate directions [Figs. 1(b)–1(f)] to the $d_{x^2-y^2}$ model. The broken curve represents the calculated conductance curve taking into account the broadening of the one-electron level.

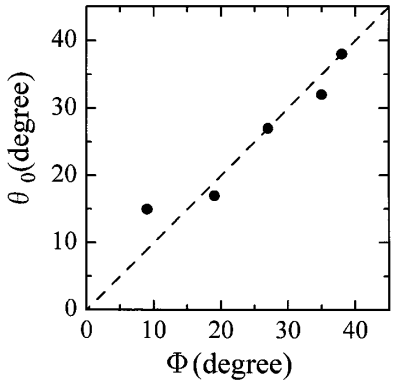

FIG. 4. Fitting parameter θ_0 against Φ. The linear relation between θ_0 and Φ indicates that the line node of the gap is at the [110] direction.

curves observed along the directions intermediate between [100] and [110] are well explained by the $d_{x^2-y^2}$-wave gap.

Shen *et al.* [2] observed the gap maximum along the [100] direction and observed the vanishing of the gap along the [110] direction in ARPES measurements on $Bi_2Sr_2CaCu_2O_8$ single crystals. The similar result was reported by Yokoya and Takahashi [3]. Although the existence of node is not ensured owing to the limit of the energy resolution, these results are consistent with ours. On the other hand, Kane and Ng [9] observed the gap minimum about 20 meV along near the [100] direction and observed the gap maximum about 35 meV along near the [110] direction, in STM spectroscopy on $Bi_2Sr_2CaCu_2O_8$ single crystals. At first sight, this result seems to indicate the d_{xy}-wave symmetry and seems to be inconsistent with our result, which indicates the $d_{x^2-y^2}$-wave symmetry. We do not know the cause of this $\pi/4$ difference yet. However, the gap value is sample dependent, as described above. We think that our conclusion based on the functional form of conductance curves is highly conclusive.

As shown in Fig. 1, the so-called zero-bias conductance peak (ZBCP) structure [17] was observed along the [100] direction, and a clear superconducting gap structure was observed along the [110] direction. The ZBCP structure was reported also by other groups for the tunneling spectroscopy measurements on high-T_c cuprates [5–7,18–20]. It is claimed that the ZBCP is due to line nodes on the Fermi surface of the d-wave superconducting gap [17,21–23]. According to these theories, these results seem to suggest the d_{xy}-wave gap and be inconsistent with the results along the directions intermediate between [100] and [110] at first sight. However, these curves observed along the [100] and [110] directions are also explained by the $d_{x^2-y^2}$-wave gap, taking into account the electron orbital in the periodic arrangement of surface oxygen atoms in the Cu-O plane [6]. This was already discussed in detail in our previous paper [14].

In conclusion, we have investigated the gap structure in the superconducting phase of $Bi_2Sr_2CaCu_2O_8$ by STM spectroscopy measurement and observed angular dependent tunneling differential conductance curves. The curves observed along the directions intermediate between [110] and [100] are well fitted with the $d_{x^2-y^2}$-wave gap model, taking into account the **k** dependence of the tunneling transition probability. This strongly indicates that the pair wave function has the $d_{x^2-y^2}$-wave symmetry.

The authors would like to thank Professor F. J. Ohkawa and Professor M. Oda for valuable discussions.

[1] W. N. Hardy, D. A. Bonn, D. C. Morgan, Ruixing Liang, and Kuan Zhang, Phys. Rev. Lett. **70**, 3999 (1993).
[2] Z. X. Shen, D. S. Dessau, B. O. Wells, D. M. King, W. E. Spicer, A. J. Arko, D. Marshall, L. W. Lombardo, A. Kapitulnik, P. Dickinson, S. Doniach, J. DiCarlo, A. G. Loeser, and C. H. Park, Phys. Rev. Lett. **70**, 1553 (1993).
[3] T. Yokoya and T. Takahashi, Solid State Commun. **87**, 553 (1993).
[4] P. C. Hammel, M. Takigawa, R. H. Heffner, Z. Fisk, and K. C. Ott, Phys. Rev. Lett. **63**, 1992 (1989).
[5] L. Alff, H. Takashima, S. Kashiwaya, N. Terada, H. Ihara, Y. Tanaka, M. Koyanagi, and K. Kajimura, Phys. Rev. B **55**, 14 757 (1997).
[6] S. Tanaka, E. Ueda, M. Sato, K. Tamasaku, and S. Uchida, J. Phys. Soc. Jpn. **64**, 1476 (1995).
[7] J. Y. T. Wei, N.-C. Yeh, D. F. Garrigus, and M. Strasik, Phys. Rev. Lett. **81**, 2542 (1998).
[8] C. Manabe, M. Oda, and M. Ido, J. Phys. Soc. Jpn. **66**, 1776 (1997).
[9] J. Kane and K.-W. Ng, Phys. Rev. B **53**, 2819 (1996).
[10] Ch. Renner and Ø. Fischer, Phys. Rev. B **51**, 9208 (1995).
[11] H. Murakami and R. Aoki, J. Phys. Soc. Jpn. **64**, 1287 (1995).
[12] Y. DeWilde, N. Miyakawa, P. Guptasarma, M. Iavarone, L. Ozyuzer, J. F. Zasadzinski, P. Romano, D. G. Hinks, C. Kendziora, G. W. Crabtree, and K. E. Gray, Phys. Rev. Lett. **80**, 153 (1998).
[13] K. Ichimura, K. Suzuki, K. Nomura, and S. Takekawa, J. Phys. Condens. Matter **7**, L545 (1995).
[14] K. Suzuki, K. Ichimura, K. Nomura, and S. Takekawa, J. Phys. Condens. Matter **11**, 3133 (1999).
[15] E. L. Wolf, *Principles of Electron Tunneling Spectroscopy* (Oxford University Press, New York, 1989), p. 21.
[16] K. Ichimura, T. Arai, K. Nomura, S. Takasaki, J. Yamada, S. Nakatsuji, and H. Anzai, Physica (Amsterdam) **282C–287C**, 1895 (1997).
[17] Chia-Ren Hu, Phys. Rev. Lett. **72**, 1526 (1994).
[18] Saion Shinha and K.-W. Ng, Phys. Rev. Lett. **80**, 1296 (1998).
[19] M. Covington, M. Aprili, E. Paraoanu, L. H. Greene, F. Xu, J. Zhu, and C. A. Mirkin, Phys. Rev. Lett. **79**, 277 (1997).
[20] M. Taira, M. Suzuki, Xu-Guang Zheng, and T. Hoshino, J. Phys. Soc. Jpn. **67**, 1732 (1998).
[21] M. Matsumoto and H. Shiba, J. Phys. Soc. Jpn. **64**, 1703 (1995).
[22] Y. Tanaka and S. Kashiwaya, Phys. Rev. Lett. **74**, 3451 (1995).
[23] M. Fogelström, D. Rainer, and J. A. Sauls, Phys. Rev. Lett. **79**, 281 (1997).